JOURNAL OF CATALYSIS 102, 80–91 (1986)

Model CO_2 Gasification Reactions on Uncatalyzed and Potassium Catalyzed Glassy Carbon Surfaces

S. R. KELEMEN AND H. FREUND

Corporate Research Laboratories, Exxon Research and Engineering Laboratories, Clinton Township, Rte. 22 East Annandale, New Jersey 08801

Received January 23, 1986; revised June 10, 1986

The individual steps in the uncatalyzed and potassium catalyzed CO_2 gasification reaction were studied on glassy carbon surfaces using Temperature-programmed reaction spectroscopy (TPRS) with labeled isotopes, Auger electron spectroscopy (AES), and steady-state reaction kinetics. Uncatalyzed CO_2 gasification surfaces showed the presence of strongly bound oxygen. Subsequent CO_2 adsorption and dissociation activity were severely limited on uncatalyzed surfaces. In contrast, potassium catalyzed glassy carbon surfaces were active for CO_2 adsorption and dissociation. The energy barrier for dissociation of CO_2 to yield adsorbed oxygen and gaseous CO was estimated at 28 kcal/mole on the potassium catalyzed glassy carbon surface. Our results show that while the energetics of the CO formation step to produce CO from lattice carbon control the energetics of gasification by CO_2, the dissociative adsorption step is responsible for the increase in reaction site density and increased gasification rate.

INTRODUCTION

The empirical identification of carbon gasification catalysts has yielded to a more focused effort to understand the mechanisms of carbon gasification. Potassium catalyzed CO_2 and H_2O carbon gasification system have received by far the most attention (*1–21*). The efforts have yielded sufficient information to describe the mode of catalyst formation and catalytic action on a wide variety of reactant carbons. Catalyst precursor complexes can be formed from the reaction of potassium salts with carbon surfaces (*2, 3*). The presence of oxygen containing functionalities on the carbon surface facilitate catalyst formation (*21*). Potassium complexes are well dispersed on carbon. The potassium complex is associated with oxygen on carbon (*5, 8, 12, 14, 19–21*). The complex takes part in the catalytic cycle by way of an oxygen transference mechanism. Despite these findings it is still difficult to assemble and quantify the explicit chemical pathway of the catalytic reaction. A knowledge of the mechanism of the uncatalyzed carbon gasification reaction is an essential component to achieve a description of catalytic action. It is equally important to consider the carbon type in a full description of the catalytic process as the nature of the substrate carbon can modify to some extent the precise surface chemistry.

Kinetic studies of uncatalyzed (*22–24*) and potassium catalyzed (*25*) carbon gasification systems have demonstrated that a classical oxygen exchange mechanism can be applied to these systems. An increase in the rate of product formation is generally observed with the addition of potassium catalysts, yet the energetics of the overall reaction remain nearly constant for a given carbon type (*25*). Catalytic operation along these lines has been interpreted in terms of an increase in "active" site density (*25, 26*). Our approach to understand the mechanism of catalytic action has been to apply surface characterization techniques to kinetically well-defined carbon gasification systems. In the case of the uncatalyzed CO_2 gasification reaction we have concentrated our efforts on a "paracrystalline" glassy carbon (*27*). The quantitative aspects of

0021-9517/86 $3.00

how the presence of a potassium catalyst increases the number of active sites for CO_2 gasification of glassy carbon is the subject of the present work. Surface sensitive probes which include temperature-programmed reaction spectroscopy (TPRS) have been successfully applied in potassium catalyst characterization studies (*14*). These methods can be extended to model gasification systems where the gas dissociation step can be separately studied from the product CO formation step.

II. EXPERIMENTAL

The glassy carbon starting material was obtained as plates from Atomergic Chemetals. Samples were made in the form of powders and chips. Powders (60–80 mesh) were produced by grinding and sieving glassy carbon plates. Powders were found to have 5 m^2/g specific surface area based on Kr chemisorption measurements. Powdered samples were used in steady-state kinetic studies and temperature-programmed experiments. The reaction kinetics were done in a Dupont Model 951 thermogravimetric analyzer (TGA). Fifty milligrams of material was the normal sample size. Uncatalyzed glassy carbon powders were first heated up to 900°C in argon prior to experiments. Potassium catalysts could be produced in several ways. A physical mixture of K_2CO_3 and carbon heated to 800°C in an inert environment is a standard method used in the study of steady-state kinetics of carbon (*25*). Another method of preparation, which yielded comparable steady-state kinetic results, was by ion exchange using a KOH solution added to HNO_3 preoxidized glassy carbon (*21*). These potassium-treated samples were heated in argon to 800°C prior to experiments. Thermal treatment decomposed the initial acid sites and yielded a well-dispersed submonolayer concentration of potassium catalyst on the glassy carbon surface. This procedure minimized complications due to the presence of excess bulk potassium salts. Kinetic data for the uncatalyzed and potassium catalyzed reactions we obtained under steady-state conditions over the range of 1–15% burn-off.

The TPRS apparatus used with powdered samples was specially constructed as an appendage to a UHV spectroscopy chamber which housed quadrupole mass spectrometers. The TPRS unit had a base pressure of 5×10^{-10} Torr pumped separately by a Balzers 300 liter/s turbomolecular pump. Samples of 5–10 mg were accommodated in a ceramic vessel 9 mm long × 3 mm diameter. A Chromel–Alumel thermocouple was inserted into the sample bed. The sample holder was resistively heated by tantalum elements and the sample temperature was controlled by a Micristar controller. The volume of the TPRS apparatus was approximately 100 cm^3 and gas dosing was accomplished via direct gas introduction by way of a Granville Phillips variable leak valve connected to a gas manifold.

The glassy carbon chips were cut from plates with a diamond saw to 1 cm × 1 cm × 1 mm dimensions. The chips were washed with deionized water and then outgassed to ~1000°C in UHV prior to use. The specific surface area of the chips were 0.3 m^2/g based on Kr chemisorption measurements. The samples were not designed for detailed kinetic measurements, but these chips experienced the same reaction conditions as the powdered samples. The chips were especially suited for use in a atmospheric pressure/UHV sample introduction system. Samples could be given reactive treatment up to 750°C in 1 atm gas and returned into a UHV apparatus for surface analysis without exposure to air. Glassy carbon chips as well as powdered samples which received kinetic analysis in the TGA apparatus and which were cooled to room temperature in the reactant gas mixture, could be transferred in atmosphere to respective holders for TPRS experimentation. Brief exposure to air at room temperature did not alter reactivity patterns observed in subsequent steady-state kinetic experiments.

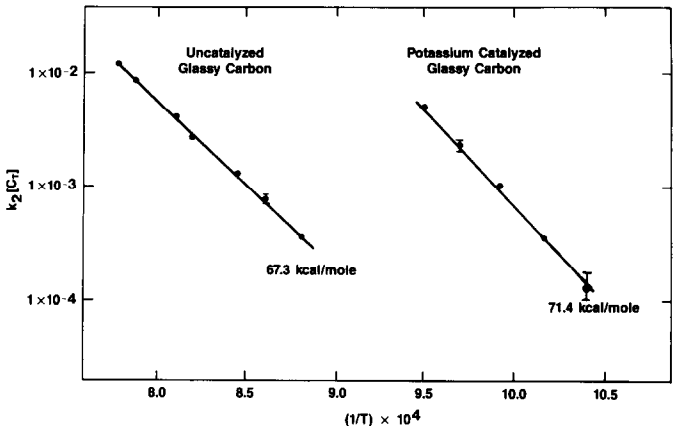

FIG. 1. Arrhenius plots for uncatalyzed and potassium catalyzed CO_2 gasification of glassy carbon powder.

Auger electron spectroscopy (AES) was performed with a grazing incidence electron gun and a Physical Electronics double pass CMA. The chamber was equipped with both an EAI and an Extranuclear quadrupole mass spectrometer. The EAI unit had dual mass scanning capability during a TPRS experiment while the Extranuclear spectrometer, interfaced to a PDP 11 data acquisition system, provided the capability to follow up to 11 masses during a TPRS experiment.

The CO_2 used was research purity obtained from Matheson gas products CO_2 (99.995%), O_2 (3 ppm). CO_2 was further purified of O_2 in TGA experiments by passing the gas over a Spherocarb bed held at 700°C to convert O_2 to CO. $^{13}CO_2$ was obtained at 99% enrichment from Isotec, Inc. $^{13}C^{18}O_2$ was obtained from Stohler Isotope Chemicals at a 95% enrichment level.

III. RESULTS

The CO_2 gasification kinetics of glassy carbon were studied and analyzed in the context of the classical oxygen exchange mechanism (*28*)

$$C(f) + CO_2 \underset{k-1}{\overset{k_1}{\rightleftharpoons}} C(O) + CO \qquad (1)$$

$$C(O) \xrightarrow{k_2} CO + C(f) \qquad (2)$$

where C(f) is an available active site, C(O) is an occupied site, and C(f) + C(O) = C_T. The steady-state assumption is applied to C(O) and the resulting rate expression is given as

$$R = \frac{k_1[CO_2][C_T]}{1 + k_{-1}/k_2[CO] + k_1/k_2[CO_2]}. \qquad (3)$$

Under modest gasification conditions the rate expression reduces to (*28*)

$$R = \frac{k_2[C_T]}{1 + [CO]/[CO_2]K_{eq}}. \qquad (4)$$

K_{eq} is the equilibrium constant for Reaction (1). This shows that the effect of CO/CO_2 ratio must be taken into account as well as K_{eq}. This has been done for a variety of carbon systems (*25*), including glassy carbon. A plot of $k_2[C_T]$ vs $1/T$ will yield a line with slope E_a/R. The results for uncatalyzed and potassium-catalyzed glassy carbon systems are shown in Fig. 1. The activation energy of the uncatalyzed system, determined by least squares analysis, was 67.3 kcal/mole. For the potassium catalyzed system a comparable value, 71.4 kcal/mole, was obtained as a best fit. As is commonly observed, there is a striking dis-

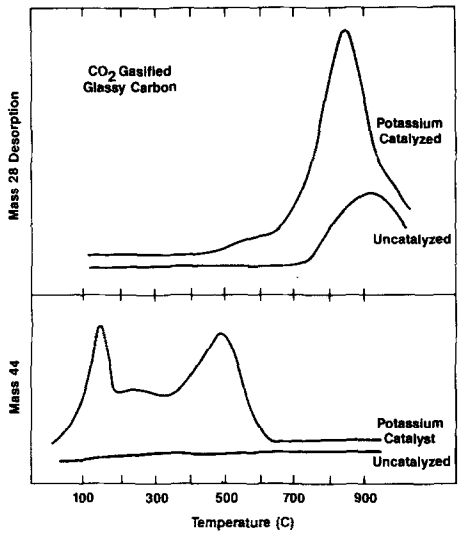

FIG. 2. A comparison of the UHV TPRS profile from uncatalyzed and potassium catalyzed glassy carbon powder samples following cooling to room temperature in the reactant gases.

parity in absolute rates for the uncatalyzed and potassium catalyzed systems.

The uncatalyzed and potassium catalyzed CO_2 gasification surfaces were examined in close detail. The glassy carbon samples were cooled in their reactant mixture to room temperature and transferred to the UHV environment for TPRS and AES analysis. A series of experiments was designed to characterize the surfaces and then probe the separate steps in the CO_2 gasification reaction.

The gasified glassy carbon samples were temperature-programmed at a rate of 1°C per second. Mass 28 and mass 44, CO and CO_2, respectively, dominated the gaseous evolution. Figure 2 shows typical results observed with uncatalyzed and potassium catalyzed samples. There is a large amount of CO_2 evolved from the catalyzed sample up to 600°C. There are two prominent peaks which occur near 150 and 500°C. In contrast to this situation, there is over an order of magnitude less CO_2 evolved from the uncatalyzed sample. CO is observed from both samples at high temperatures. The contribution to mass 28 from CO_2 cracking in the mass spectrometer ionizer has been subtracted from each spectrum. In the case of the catalyzed reaction, CO evolution begins at 500°C and extends over the next 450°C. CO evolution has still not returned to baseline at the end of the experiment at 950°C. Substantial CO evolution is found with uncatalyzed samples. The total amount of CO is approximately one-third that from the potassium-catalyzed surface. CO is first detected near 700°C, 200°C higher than the catalyzed case. The complexity of the gas evolution from both samples indicate that there are several processes at work.

CO production at high temperatures from uncatalyzed glassy carbon surfaces has been previously examined in some detail (*27*). CO formation originates from lattice carbon. The wide range of temperature for production has been interpreted in terms of coverage dependent reaction energetics. This behavior was also observed with O_2 oxidation of glassy carbon and edge graphite surfaces. In the case of CO_2 gasification of glassy carbon almost all of the CO evolution is representative of strongly held oxygen. Estimates for the CO formation energies range from 75 to 90 kcal/mole going from the highest to the lowest surface coverages (*27*). This kind of oxygen also appears to be a component of the potassium catalyzed surface. The contention of increasing CO formation energetics with decreasing oxygen coverage is supported by the following experiment. A potassium-catalyzed glassy carbon surface was temperature-programmed to a given temperature, quenched to low temperature and then reflashed to a higher temperature. The interrupt temperatures were chosen at 775, 825, and 875°C. The results are shown in Fig. 3. Curve A corresponds to the first flash. Curve B corresponds to the flash after the 775°C interrupt, Curve C to the 825°C interrupt, and Curve D after the 875°C interrupt. As a result of flash B the remaining oxygen coverage was lowered to 67% of the amount present before B. If a simple first-

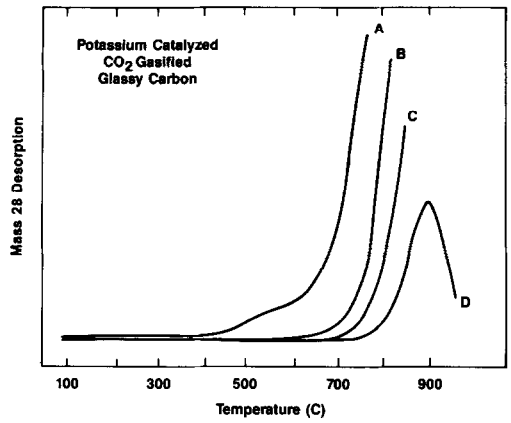

FIG. 3. CO evolution from a potassium-catalyzed glassy carbon powder sample produced by thermal processing to successively higher maximum temperatures and cooling in UHV.

order process is solely responsible for the high temperature CO evolution then the leading edge of the next flash C should reproduce the preceding flash B at approximately 67% intensity. This is not the case. The intensity of the leading edge of flash C corresponds to only 33%. The next flash interval also shows less than expected intensity from a single first-order process. After flash C the remaining oxygen coverage was lowered to 50% of the amount present before flash C. The intensity of the leading edge of flash D corresponds to only 30% of Curve C. We would anticipate CO formation to proceed via a first-order reaction since the reactant carbon is thought to have restricted mobility on the surface. These results can be rationalized if CO is produced by way of several first-order processes having kinetics with different energetics.

AES was used to characterize the amount of oxygen and potassium present on the uncatalyzed and potassium catalyzed gasification surfaces after steady-state reaction. The oxygen AES signal and the AES potassium signal normalized to the carbon substrate signal was used to measure the relative concentration changes. Consequently, these are not absolute coverage scales. Figure 4 shows the results following heating in UHV. The samples were heated to the indicated temperature for 300 s at each point. An AES O/C ratio of 0.30 corresponds to nearly a full monolayer coverage (*27*). These results clearly show that the majority of oxygen-containing species are lost upon heating above 900°C in UHV. Separate experimental runs show that atomically clean surfaces are in fact recovered upon heating just above 1000°C with only trace levels of oxygen contamination. The relative changes in magnitude of the oxygen signals for the catalyzed and uncatalyzed surfaces correspond with the relative amounts and changes in CO produced in TPRS experiments from these surfaces. Decreases occur at slightly lower temperatures in the AES experiments relative to the TPRS experiments due to the much longer heating times. The potassium catalyzed

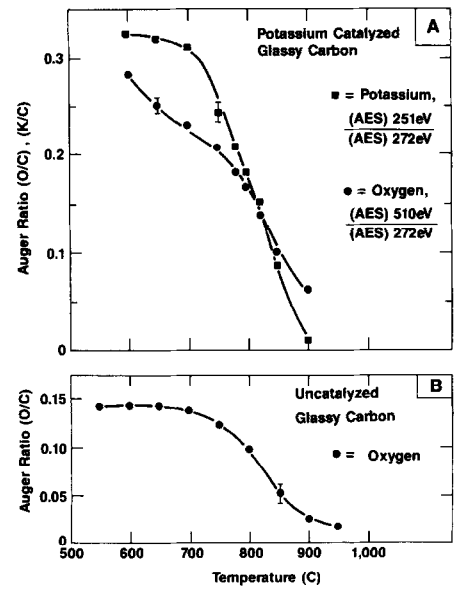

FIG. 4. Catalyzed and uncatalyzed samples were cooled from reaction conditions to room temperature in the reactant gases. (A) Change in the AES O/C ratio on the uncatalyzed glassy carbon surface after heating for 300 s at each point in UHV. (B) Changes in the AES O/C and K/C ratio on the potassium catalyzed glassy carbon surface after heating for 300 s at each point in UHV.

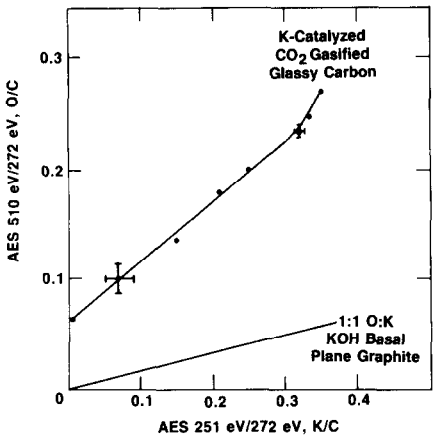

FIG. 5. A potassium catalyzed sample was cooled from reactive conditions. The changes in the AES oxygen signal relative to potassium followed upon heating in UHV. The result for KOH desorption from the basal surface of graphite is included as a calibration.

surfaces show a much greater decrease in oxygen AES signal below 700°C relative to the uncatalyzed surface. Up to 700°C, the potassium signal is nearly constant. This observation is consistent with previously reported thermal stability observations for potassium catalysts (*8, 20*). Potassium can be vaporized at higher temperatures. In inert environments, there is a precipitous decline in the potassium AES signal between 750 and 850°C. This behavior is also consistent with the observed stability in other systems (*21, 29*).

The AES oxygen signal, O/C, was tabulated relative to the potassium signal, K/C, for the UHV thermal experiments just described. The results are shown in Fig. 5. The AES signal response for KOH desorption is the monolayer regime (*30*), a compound with 1:1, O:K stoichiometry, is also shown as a calibration. Based on this calibration, the monolayer surface composition of the potassium-catalyzed surface shows a 4:1, O:K relative stoichiometry. Decreases in the potassium Auger ratio scale with the oxygen ratio. As CO is produced into the gas phase, potassium is vaporized from the surface. Upon heating to temperatures above 900°C the potassium signal disappears yet there is still a small AES O/C ratio. This represents very strongly bound residual oxygen. At typical gasification temperatures, 700–800°C, the potassium catalyst exists on the carbon surface in an excess "sea" of oxygen.

Heating to 800°C in UHV showed that submonolayer concentrations of potassium catalyst and oxygen could still be maintained. Exposure of these surfaces to CO_2 and subsequent TPRS experiments show that these surfaces were active for CO_2 adsorption at 300°C. Repetitive thermal cycling encountered in TPRS experiments caused the gradual loss of potassium catalyst and CO_2 adsorption capacity. This behavior is shown by the results in Fig. 6. The CO_2 evolution, mass 44, is monitored as a function of temperature for a heating rate of 1°C/s. Curve A corresponds to the initial potassium catalyzed gasification sample cooled from reaction temperature in CO_2. Peaks occur near 150 and 475°C. The maximum sample temperature during the TPRS run was 825°C. Curve B was produced after the first TPRS run by exposing the sample to 1 atm CO_2 at 300°C, allowing the sample

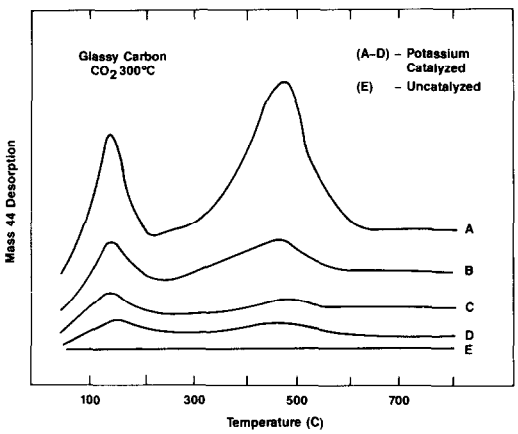

FIG. 6. CO_2 TPD mass 44 from a potassium-catalyzed surface following: curve A cooling in CO_2 from gasification conditions; curve B after curve A and 1 atm CO_2 at 300°C; curve C after curve B and 1 atm CO_2 at 300°C; curve D after curve C and 1 atm CO_2 at 300°C; curve E after curve D and 1 atm CO_2 at 300°C.

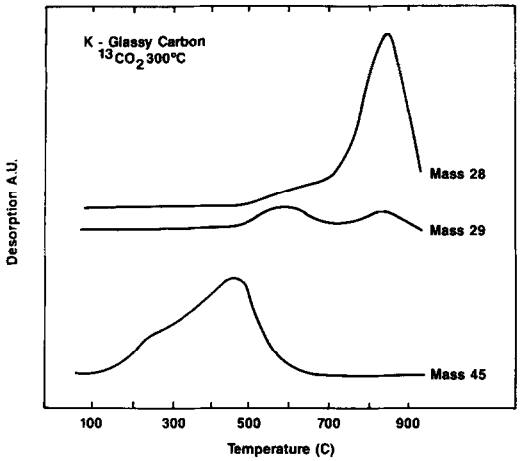

FIG. 7. TPRS profile following 1 atm $^{13}CO_2$ exposure at 300°C to a glassy carbon surface containing the potassium catalyst. The catalyzed surface was first heated in UHV.

to cool to room temperature in CO_2 and then evacuating the sample to 10^{-9} Torr. The CO_2 evolution from this experiment follows a similar pattern as observed directly following catalyzed CO_2 gasification. The amount of CO_2 declines with the decreased level of potassium catalyst. This cycle was repeated in Curves C and D. The same pattern of CO_2 evolution is found and there is a continued decline in the amount of CO_2 produced as the potassium catalyst concentration drops further as a result of the multiple heating cycles to 800°C. For comparison, Curve E shows the same experiment with uncatalyzed glassy carbon where virtually no CO_2 adsorbs under these conditions. The results demonstrate the CO_2 absorption capacity is linked to the concentration of potassium catalysts on the glassy carbon surface.

The CO_2 adsorption step is only partially reversible. On potassium catalyzed surfaces isotopically labeled CO_2 adsorption studies were carried out to probe the gas dissociation step to produce gaseous CO and adsorbed oxygen. The potassium catalyzed surface was first heated to 780°C in UHV. The TPRS experiment was done following $^{13}CO_2$ exposure at 1 atm gas pressure and the sample held at 300°C. The gas was removed at 300°C and the sample allowed to cool while pumping. The results of the TPRS experiment are shown in Fig. 7. $^{13}CO_2$ mass 45, ^{13}CO mass 29, and ^{12}CO mass 28 were the dominant gaseous products. $^{13}CO_2$ desorption signal was comparable to previous results for CO_2 except for the lack of a 150°C desorption peak which is expected since the sample was cooled under vacuum in this experiment. Mass 45 desorption occurred over several hundred degrees with a peak maximum near 475°C. The large quantity of $^{13}CO_2$ observed indicates that the adsorption processes are largely reversible.

There is evidence that a portion of $^{13}CO_2$ dissociates during exposure at 300°C. ^{13}CO desorbs above 500°C. There are two peaks in the spectrum which occur near 575 and 850°C. The ^{13}CO peak at 575°C indicates that $^{13}CO_2$ dissociates to give adsorbed oxygen and gaseous ^{13}CO. Mass 28 CO desorption also occurs from this system and must originate from lattice carbon. $^{13}CO_2$ adsorption happens on the potassium catalyzed surface that possesses a sizable standing population of adsorbed oxygen species. The 800°C initial heat treatment is not sufficient to remove all of the surface oxygen nor all of the potassium catalyst. We expect that an amount of oxygen comparable to the amount of labeled CO will be added to the standing oxygen population. The desorption of CO from lattice carbon begins above 700°C and proceeds to higher temperatures. The presence of additional oxygen in the standing population manifests itself in increased CO production at the lower temperature end of the CO manifold (see Fig. 3). The added CO production from lattice carbon does not give rise to a "clean" desorption peak but rather contributes to a wide distribution. ^{13}CO is also evident in the high temperature distribution of carbon monoxide. Some labeled carbon from the gaseous reactant exchanges with the carbon substrate during the course of reaction.

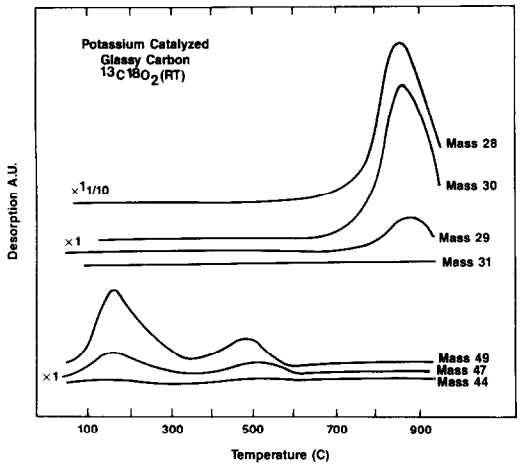

FIG. 8. TPRS profile following 100 Torr $^{13}C^{18}O_2$ exposure at room temperature to a glassy carbon surface containing the potassium catalyst. The catalyzed surface was first heated in UHV.

CO_2 adsorption and dissociation are activated processes on potassium catalyzed glassy carbon. TPRS studies following room temperature $^{13}C^{18}O_2$ adsorption at reduced pressure illustrate this point (see Fig. 8). Only a small amount of $^{13}C^{18}O_2$ adsorbs following a 15-min exposure to $^{13}C^{18}O_2$ at 100 Torr pressure. Mass 28 originating from the standing initial oxygen population is the dominant high temperature desorption peak. The low temperature peak is now relatively larger than the 475°C peak as the high temperature state is only partially filled. Mass 47 is a one-third contribution to the total carbon dioxide signal and there is almost no mass 44 CO_2. Carbon dioxide exchanges oxygen with the standing oxygen population on the carbon surface, as evidenced by a significant mass $^{12}C^{18}O$ component at higher temperatures. Carbon from $^{13}C^{18}O_2$ does not readily exchange with the substrate carbon under these conditions. $^{13}C^{18}O_2$ does not dissociate yielding gaseous $^{13}C^{18}O$ under the present conditions as evidenced by an absence of a 575°C peak.

In order to probe the energy barrier for CO_2 dissociation on the catalyzed surface, we have measured the increase in the oxygen Auger signal as a function of exposure to CO_2 with the sample held at 500°C. The samples were first heated to 750°C in UHV. The initial AES K/C ratio was 0.15 which remained constant during the experiment. The results are shown in Fig. 9. The uncatalyzed surface produces no measurable increase in oxygen signal for these conditions. On the other hand, the catalyzed surface shows an oxygen signal increase beyond 10^6 (L) exposure. The signal continues to rise over the next several decades and then begins to level off. CO_2 desorption is not observed following these conditions indicating that CO_2 irreversibly dissociates on the potassium catalyzed glassy carbon surface.

IV. DISCUSSION

Previous studies which have concentrated on the kinetics of uncatalyzed and potassium catalyzed carbon gasification by CO_2 have contributed to a mechanistic description of the reaction. For a given reactant carbon, the rate increases with catalyst addition but the activation energy remains almost constant (*25*). This behavior was also found in the study of glassy carbon. On glassy carbon an activation energy of 69 ± 4 kcal/mole was determined by way of the

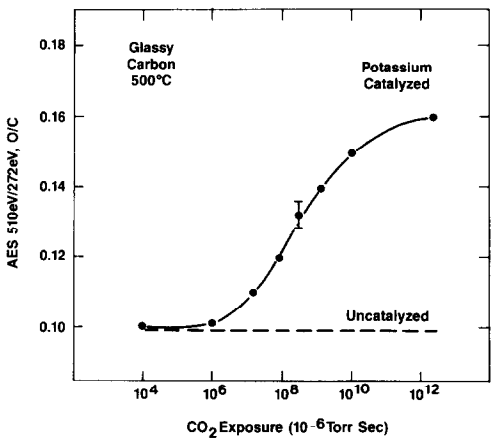

FIG. 9. Increase in the oxygen AES O/C ratio as a function of exposure to CO_2. The catalyzed and uncatalyzed samples were heated to 750°C in UHV prior to CO_2 exposure. The surface temperature was held at 500°C.

classical oxygen exchange mechanism. Observations such as this are the basis for the conclusion that the potassium catalyst acts to increase the concentration of active carbon sites. The precise chemical pathway responsible for this action has not been previously addressed. We have characterized uncatalyzed and potassium catalyzed glassy carbon surfaces with surface sensitive spectroscopies as well as followed adsorption desorption processes in order to quantify the aspects of carbon gasification catalysis.

Potassium catalyzed surfaces heated in UHV to reaction temperatures are distinguished in the ability to adsorb and subsequently dissociate CO_2. Reversible CO_2 adsorption is characterized by a desorption maximum of 475°C, while dissociation to produce gaseous CO and the oxygen surface species is marked by a 575°C ^{13}CO peak in $^{13}CO_2$ studies. We can obtain a rough idea of the energetics of these processes from the desorption peak temperature maximum if we assume first-order kinetics with preexponential factor of 10^{13}. This estimate yields a value of 48 kcal/mole for CO_2 desorption and 55 kcal/mole for dissociation. The increase in the oxygen AES signal as a function of CO_2 exposure with the glassy carbon surface held at 500°C can provide information about the energetics of direct gas dissociation. We can determine from experimental data the probability of a successful dissociation event under these conditions ($\sim 10^{-8}$–10^{-10}). If we assume a Boltzmann energy distribution and a CO_2 gas temperature equivalent to the surface temperature, then the energy barrier for gas dissociation is of the order of 28 kcal/mole.

The energetics of the CO formation step to produce CO from lattice carbon control the energetics of the gasification reaction. AES characterization of CO_2 gasification surfaces quenched in reactant gases shows that the overall surface oxygen concentration on the uncatalyzed surface is nearly half that of the potassium catalyzed surface. Heating in UHV to elevated temperature shows that both surfaces have significant large standing populations of very stable oxygen. In addition to this kind of oxygen, the potassium catalyzed surface exhibits loss in the form of CO at lower temperatures. TPRS results of CO at high temperatures demonstrate that CO is not produced by way of simple first-order kinetics. A range of CO formation energetics must be postulated to account for the CO TPRS evolution. Insight into CO formation energetics on glassy carbon surfaces was detailed in a previous comparative study of CO_2 and O_2 oxidation (*27*). It was found that a relatively large standing population of surface oxygen existed with subsequent CO formation energetics >75 kcal/mole. O_2 demonstrated a vastly greater capacity to dissociate on surfaces at high oxygen coverages which in turn generated CO with energetics <70 kcal/mole. CO_2 was limited in its capacity to perform this function. There is a correspondence between the activation energy for CO_2 gasification of glassy carbon determined from steady-state kinetics and the value for CO formation energetics at high oxygen surface coverages (*25*, *27*). This correspondence is anticipated since this reaction step dominates the kinetic expression of the oxygen exchange mechanism under mild gasification conditions (*28*). The energy barrier for gas dissociation increases as a function of surface oxygen coverage. The higher gasification rate, which is always observed for O_2 relative to CO_2, is associated with a more facile gaseous dissociation step at high oxygen coverages, which in turn is responsible for the generation of increased numbers of CO formation sites with lower energetics (*27*).

In some respects enhancement in CO formation from the potassium catalyzed CO_2 gasification reaction is similar to O_2 reaction under milder conditions. The presence of potassium catalyst facilitates CO_2 dissociative adsorption which results in increased surface oxygen concentration. The presence of high oxygen surface concentra-

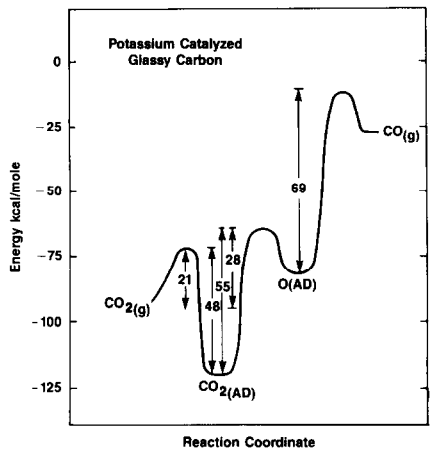

FIG. 10. Estimated energy-reaction coordination diagram for CO_2 reaction with potassium catalyzed glassy carbon.

tions is linked with lower subsequent CO formation energetics. The catalyst's ability to repopulate the carbon surface with more oxygen at already high surface oxygen concentrations is associated with increased numbers of CO formation sites with low energetics, ~70 kcal/mole.

The rough estimates of the energetics for the individual steps in the potassium catalyzed CO_2 gasification reaction can be combined in the form of an energy reaction coordinate diagram. The diagram is shown in Fig. 10 and pertains to a high oxygen coverage surface situation as representative of the actual steady-state gasification surface. The estimates are strictly associated with glassy carbon as values will be modified by the nature of the reactant carbon substrate (*25*). From the values of the barrier for direct CO_2 dissociation and the barrier for dissociation by way of an adsorbed intermediate, we can deduce a 21 kcal/mole barrier for nondissociative CO_2 adsorption on the potassium catalyzed surface. This derived value is consistent with the observation of limited CO_2 adsorption following room temperature exposure. Experiments with $^{13}C^{18}O_2$ show that while adsorption is limited at low temperature oxygen exchange reactions are prevalent with the standing population of strongly bound oxygen.

Dissociation of CO_2 to generate adsorbed oxygen occurs with an energy barrier of roughly 28 kcal/mole. This is substantially lower than that estimated on a comparable uncatalyzed surface. At high oxygen coverage the barrier for CO_2 dissociation on glassy carbon is in excess of 45 kcal/mole and it is likely that the value is substantially greater over the majority of free sites at high oxygen surface coverages (*27*). The prohibitive barriers for CO_2 dissociation on uncatalyzed free sites at high oxygen surface coverages is evidenced by the results from glassy carbon surfaces quenched in CO_2 reactant gas (Fig. 2), and CO_2 oxidations at 500°C (Fig. 9). In contrast, potassium catalyzed surfaces dissociate measurable amounts of CO_2 on free carbon sites at high overall oxygen surface coverages.

Catalytic cycles involving alkali intercalates (*2, 31, 32*), bulk-like alkali surface salts (*6, 7, 11, 33, 34*), and oxidic alkali surface species (*5, 8, 18–21*) have been considered in catalyzed carbon gasification mechanisms. The observation that catalytic gasification activity can be regained after subjecting the reaction system to inert gaseous environments at reaction temperatures (*8*) does not support the view that intercalates are involved as these compounds have limited vacuum thermal stability (*35, 36*). K_2CO_3-like species on carbon have been regarded as likely forms as they are believed to be stable with respect to vaporization (*6, 7, 34*) at gasification temperatures. Catalytic cycles have been postulated on the basis of K_2CO_3-like surface species (*6, 7, 11, 33, 34*). Recent temperature-programmed desorption results with isotopically labeled reagents indicate the existence of stable potassium surface species distinct from bulk-like K_2CO_3 (*14*). AES, UPS, and XPS characterization of potassium catalyst formation (*21*) show the presence of a potassium oxygen complex distinct from bulk-like KOH, K_2CO_3, or

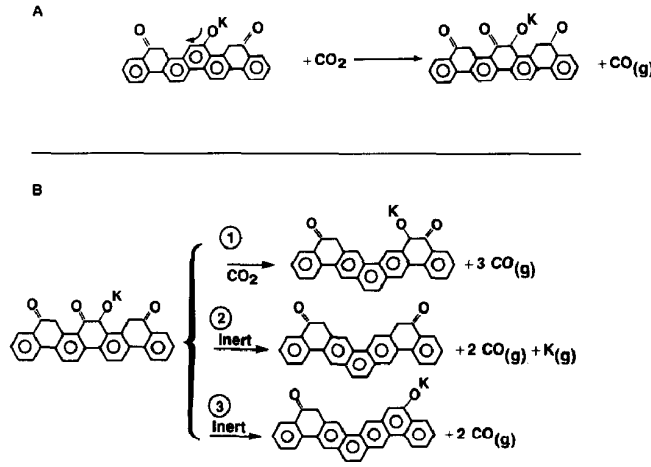

FIG. 11. (A) Proposed potassium catalyzed glassy carbon surface configuration before and after CO_2 dissociation. (B) Proposed reactions which are a result of subsequent heating in different environments, Path (1) represents an ambient of CO_2 while Paths (2) and (3) represent inert environments.

K_2O forms. Surface species of potassium and oxygen are then considered to be likely chemical forms of the potassium catalyst (*5, 8, 14, 18–21*). The presence of a surface species contained C—O—K bonds was determined by subsequent methylation of the carbon surface with CH_3I to produce C—O—CH_3 (*5, 8*). The existence of a stable surface potassium species associated with oxygen has implications in the catalyzed gasification mechanism. A catalytic cycle can be postulated which does not involve bulk-like K_2O or K_2CO_3. The observed stability of the species and ample population at gasification temperatures in inert environments indicates that the catalytic reaction involves a further reversible oxidation step involving the potassium complex (*8, 21*).

The potassium complex consists of potassium and oxygen at submonolayer concentrations. The presence of the complex modifies the surface electronic properties of carbon as seen by a decrease in work function, a trend consistent with partial charge donation to the carbon surface (*21*). The present study has focused on the oxidation step involving the potassium complex on glassy carbon surfaces and provides a basis to propose a simplified picture of the catalytic surface. The $\{11\bar{2}0\}$ "armchair" orientation is chosen for the representation in Fig. 11A, as this external edge orientation was identified to be most reactive (*9*). The presence of the catalytic potassium surface species facilitates dissociation of CO_2. The arrow in Fig. 11A indicates partial charge donation to an adjacent free carbon site. The catalyst generates an active center for gas dissociation on already heavily covered carbon surfaces. Our results suggest that, once formed, the oxidized carbon surface would undergo several possible reactions, depending on the external conditions. The proposed reactions are depicted in Fig. 11B. In the presence of ample CO_2, as found during steady-state reaction conditions, reaction one seems likely. CO is formed from lattice carbon and the potassium species is reformed on an adjacent site via reaction with CO_2 which also produces CO. Under vacuum, reactions (2) and (3) are favored. Reaction (2) involves CO formation with potassium loss. Reaction (3) involves CO formation with retention of the potassium catalyst on an adjacent oxidized site. Following reaction three the surface can be reoxidized in an ambient of CO_2, thereby continuing a catalytic cycle.

V. SUMMARY

(1) The uncatalyzed glassy carbon surface is limited in its ability to dissociate CO_2 and generate an "active" surface situation for CO formation from lattice carbon.

(2) The catalytic potassium surface species provides an active center for CO_2 adsorption and dissociation.

(3) The potassium catalyst increases the surface oxygen concentration and leads to an increase in the reaction site density relative to the uncatalyzed surface.

REFERENCES

1. Mims, C. A., and Pabst, J. K., *Amer. Chem. Soc. Dev. Fuel Chem. Prepr.* **24**(3), 258 (1980).
2. Wen, Wen-Yang, *Catal. Rev. Sci. Eng.* **22,** (1980).
3. McKee, D. W., *Chem. Phys. Carbon* **16,** 1 (1981).
4. Freiks, I. L. C., van Wechem, H. M. H., Stuiver, J. C. M., and Bouwman, R., *Fuel* **60,** 463 (1981).
5. Mims, C. A., Rose, K. D., Melchior, M. T., and Pabst, J. K., *J. Amer. Chem. Soc.* **104,** 6886 (1982).
6. McKee, D. W., *Carbon* **20,** 59 (1982).
7. McKee, D. M., Spiro, C. L., Kosky, P. G., and Lamby, E. J., *Fuel* **62,** 217 (1983).
8. Mims, C. A., and Pabst, J. K., *Fuel* **62,** 178 (1983).
9. Mims, C. A., Chludzinski, J. J., Pabst, J. K., and Baker, R. T. K., *J. Catal.* **88,** 97 (1984).
10. Wood, B. J., Brittain, R. D., and Law, K. H., *Prepr. Pap. Chem. Soc. Div. Fuel Chem.* **28**(1), 55 (1983).
11. McKee, D. W., *Fuel* **62,** 170 (1983).
12. Yuh, S. J., and Wolf, E. E., *Fuel* **62,** 252 (1983).
13. Wood, B. J., and Sancier, K. M., *Catal. Rev. Sci. Eng.* **26**(2), 233 (1984).
14. Saber, J. M., Falconer, J. L., and Brown, L. F., *J. Catal.* **90,** 65 (1984).
15. Spiro, C. L., McKee, D. W., Kosky, P. G., and Lamby, E. J., *Fuel* **63,** 686 (1984).
16. Wood, B. J., Fleming, R. H., and Wise, H., *Fuel* **63,** 1600 (1984).
17. Kapteijn, F., Abbel, G., and Moulijn, J. A., *Fuel* **63,** 1036 (1984).
18. Yuh, S. J., and Wolf, E. E., *Fuel* **63,** 1604 (1984).
19. Moulijn, J. A., Cerfontain, M. B., and Kapteijn, F., *Fuel* **63,** 1043 (1984).
20. Delannay, F., Tysoe, W. T., Heinemann, H., and Somorjai, G. A., *Carbon* **22,** 401 (1984).
21. Kelemen, S. R., Mims, C. A., and Freund, H., *J. Catal.* **97,** 228 (1986).
22. Gadsby, J., Long, F. J., Sleightholm, P., and Sykes, K. W., *Proc. R. Soc., London Ser. A* **103,** 357 (1948).
23. Mentser, M., and Ergun, S., *U.S. Bur. Mines Bull.,* 664 (1973).
24. Laurendeau, N. M., *Prog. Energy Combust. Sci.* **4,** 221 (1978) and references therein.
25. Freund, H., *Fuel* **64,** 657 (1985).
26. Otto, K., and Shelef, M., *Chem. Eng. Commun.* **5,** 223 (1980).
27. Kelemen, S. R., and Freund, H., *Carbon* **23,** 723 (1985).
28. Ergun, S. J., *J. Phys. Chem.* **60,** 480 (1956).
29. Sams, D. A., Talverdian, T., and Shadman, F., *Fuel* **64,** 1208 (1985).
30. Kelemen, S. R., and Mims, C. A., *Surf. Sci.* **133,** 71 (1983).
31. Wigmans, T., Elfring, R., and Moulijn, J. A., *Carbon* **21,** 1 (1983).
32. Wigmans, T., Haringa, H., and Moulijn, J. A., *Fuel* **62,** 256 (1983).
33. Veraa, M. J., and Bell, A. T., *Fuel* **57,** 194 (1978).
34. McKee, D. W., and Chatterji, D., *Carbon* **31,** 3811 (1975).
35. Halpin, M. K., and Jenkins, J. M., *Proc. R. Soc. London Ser. A* **313,** 421 (1969).
36. Nixon, D. E., and Parry, G. S., *J. Phys. Chem.* **2,** 1732 (1969).